Science Letters ISSN 2345-5463

Research article
2020 | Volume 8 | Issue 1 | Pages 7-17

ARTICLE INFO

Received
October 25, 2018
Revised
January 11, 2020
Accepted
January 15, 2019
Published
April 10, 2019

***Corresponding Author**
Alireza Heidari
E-mail
Alireza.Heidari@calsu.us
Central@aisi-usa.org

Keywords
Beam energy
Metal based nanoparticles
Heat distribution
Radiation therapy
Synchrotron radiation
Tumor

How to Cite
Heidari A, Schmitt K, Henderson M, Besana E. Study of human cancer cells, tissues and tumors treatment through interaction between synchrotron radiation and cerium nanoparticles. Sci Lett 2020; 8(1):7-17

Open Access

Study of Human Cancer Cells, Tissues and Tumors Treatment Through Interaction Between Synchrotron Radiation and Cerium Nanoparticles

Alireza Heidari[1, 2]*, Katrina Schmitt[1], Maria Henderson[1], Elizabeth Besana[1]

[1] Faculty of Chemistry, California South University, 14731 Comet St. Irvine, CA 92604, USA
[2] American International Standards Institute, Irvine, CA 3800, USA

Abstract

The heat transfer phenomena for single- and double-layer inclined absorbers, which absorb synchrotron radiation has been studied using analytical and numerical methods. Photon penetration through the metal layers has been included and the effects of the spectral variation of the absorption coefficients and variable thermal conductivities have been examined. Different thickness ratios and inclination angles have been studied for double layer absorbers and it has been shown that double-layer inclined absorbers significantly reduce the peak temperatures. In the current study, thermoplasmonic characteristics of cerium nanoparticles with spherical, core-shell and rod shapes were investigated. In order to investigate these characteristics, the interaction of synchrotron radiation emission as a function of the beam energy and cerium nanoparticles were simulated using the 3D finite element method. Firstly, absorption and extinction cross-sections were calculated. Then, increases in temperature due to synchrotron radiation emission as a function of the beam energy absorption were calculated in cerium nanoparticles by solving the heat equation. The obtained results showed that cerium nanorods are a more appropriate option for using in optothermal human cancer cells, tissues and tumor treatment methods. Furthermore, the produced heat devastates tumor tissues adjacent to nanoparticles without any hurt to sound tissues. Regarding the simplicity of ligands connection to cerium nanoparticles for targeting cancer cells, these nanoparticles are more appropriate to use in optothermal human cancer cells, tissues and tumors treatment.

SCAN ME

This work is licensed under the Creative Commons Attribution-Non-Commercial 4.0 International License.

Introduction

In the past ten years, synchrotron radiation generated by circulating electron or positron beams has been widely used as a powerful X-ray photon source in several fields [1–3]. Recently high energy electron or positron synchrotron storage ring to provide more brilliant and higher flux photons have been proposed and are being constructed [4–6]. The bending magnet enables electrons to circulate in the closed-loop of the storage ring and most of the photons generated should be absorbed before striking the wall of the vacuum chamber of the storage ring and the rest of those are extracted for experimental use [7]. Photon absorbers have been installed in an ultra-high vacuum storage ring to absorb unwanted photons [8]. Since synchrotron radiation generated by a high energy ring is very powerful, concentrated and penetrating, the absorber is subjected to the extremely high internal heat (comparable to that of an electron beam welding machine). Depending on the materials used, this energy generation may be restricted to the region near the surface or distributed throughout the absorber decaying exponentially in the direction of the penetration.

The cooling of the absorber is important not only to prevent the melting of the material but also to ensure an ultra-high vacuum (~/0–9torr) in a storage ring. Note that photon energy deposition in the metal causes the desorption of gases, which would result in significant increases in the pressure [9, 10]. Inclined photon absorbers have been considered in order to reduce the high wall heat flux; the inclination of the plate to the photon direction increases the photo projection area, and correspondingly, decreases the heat flux [5, 7, 11]. Since copper (Cu), which has generally been used as an absorber material absorbs most of the photons very near the surface and the temperature of the surface becomes very high despite the high thermal conductivity [12]. On the other hand, beryllium (Be), which has been widely used to isolate a storage ring from the experimental line due to its relative transparency to X–rays, diffuses the intense radiation throughout the plate, even though it has a much lower thermal conductivity than copper [13, 14]. To combine the merits of Be and Cu, a Be–Cu composite cylinder has been developed and successfully used [15]. The heat transfer of single or multilayers caused by the absorption of photons has been studied with applications to laser processing and composite materials [16]. In the present work, inclined single- and double-layer absorbers are analyzed and analytical and numerical solutions are obtained. The effects of the variable absorption coefficient of the metal, which is dependent on the photon spectrum and variable thermal conductivity are examined for different materials. In addition, the effects of different thickness ratios and different inclination angles are also studied for the double layer absorber. The present approach can also be applied to other fields; *e.g.*, laser processing and heat transfer in composite materials.

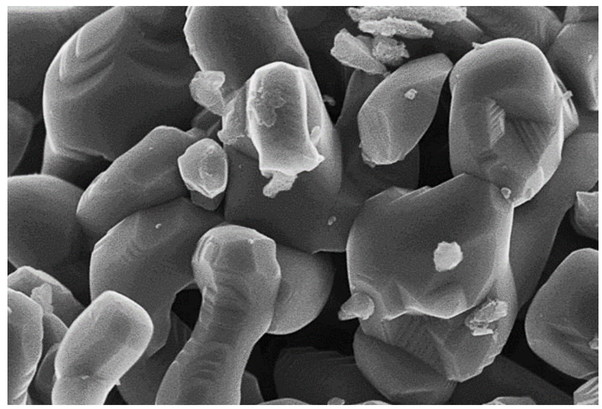

Fig. 1 Scanning electron microscope (SEM) image of cerium nanoparticles with 50000×.

In the recent decade, metallic nanoparticles have been widely interested, due to their interesting optical characteristics [1–8]. Resonances of surface plasmon in these nanoparticles lead to an increase in synchrotron radiation emission as a function of the beam energy scattering and absorption in related frequency [9, 10]. Synchrotron radiation emission as a function of the beam energy absorption and induced produced heat in nanoparticles has been considered as a side effect in plasmonic applications for a long time [11–15]. Recently, scientists found that thermoplasmonic characteristics can be used for various optothermal applications in cancer, nanoflows and photonic [17–22]. In optothermal human cancer cells, tissues and tumor treatment, the descendent laser light stimulates resonance of surface plasmon of metallic nanoparticles and as a result of this process, the absorbed energy of descendent light converse to heat in nanoparticles [23–25]. The produced heat devastates tumor tissue adjacent to nanoparticles without any hurt to sound tissues [26-29]. Regarding the simplicity of ligands connection to cerium nanoparticles (Fig. 1) for targeting cancer cells, these nanoparticles are more appropriate to use in optothermal human cancer cells, tissues and tumor treatment [30–74]. In the current paper, thermoplasmonic characteristics of spherical, core-shell and rod cerium nanoparticles are investigated.

Materials and Methods

To calculate the generated heat in cerium nanoparticles, COMSOL software, which works by Finite Element Method (FEM) was used. All simulations were made in 3D. Firstly, absorption and scattering cross-section areas were calculated by the optical module of the software. Then, using the heat module, temperature variations of nanoparticles and its surrounding environment were calculated with data from the optical module [94–99]. In all cases, cerium nanoparticles are presented in water environment with dispersion coefficient of 1.84 and are subjected to flat wave emission with linear polarization. The intensity of the descendent light was 1 mW/μm^2. The dielectric constant of cerium is dependent on particle size [100–114]. It should be noted that here descendent light means synchrotron radiation (also known as magnetobremsstrahlung radiation) is the electromagnetic radiation emitted when charged particles are accelerated radially, *e.g.*, when they are subject to an acceleration perpendicular to their velocity ($a \perp v$). It is produced, for example, in synchrotrons using bending magnets, undulators and/or wigglers. If the particle is non–relativistic, then the emission is called cyclotron emission. If, on the other hand, the particles are relativistic, sometimes referred to as ultrarelativistic, the emission is called synchrotron emission [1]. Synchrotron radiation may be achieved artificially in synchrotrons or storage rings, or naturally by fast electrons moving through magnetic fields. The radiation produced in this way has a characteristic polarization and the frequencies generated can range over the entire electromagnetic spectrum which is also called continuum radiation.

Heat generation in synchrotron radiation emission

When cerium nanoparticles are subjected to descendent light, a part of light scattered (emission process) and the other part absorbed (non–emission process). The amount of energy dissipation in non–emitting process mainly depends on the material and volume of nanoparticles and it can be identified by the absorption cross-section. On the other hand, the emission process whose characteristics depends on volume, shape and surface characteristics of nanoparticles are explained by scattering cross-section. The sum of absorption and scattering processes that lead to light dissipation is called extinction cross-section [75–85].

Cerium nanoparticles absorb the energy of descendent light and generate some heat in the particle. The generated heat transferred to the surrounding environment and leads to an increase in temperature of adjacent points to nanoparticles. Heat variations can be obtained by the heat transfer equation [86–93].

Results and Discussion

Firstly, calculations were made for cerium nanospheres with a radius of 5, 10, 15, 20, 25, 30, 35, 40, 45 and 50 nanometers. The results show that by the increase in nanoparticles size, extinction

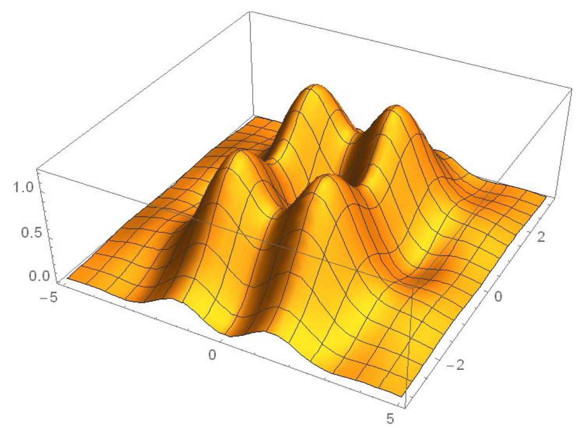

Fig. 2 Maximum increase in temperature for cerium nanospheres. It should be noted that x-axis shows cerium nanospheres radius (nanoparticles size) (nm), y–axis shows temperature of nanospheres in surface plasmon frequency (K) and z-axis shows wavelength (nm).

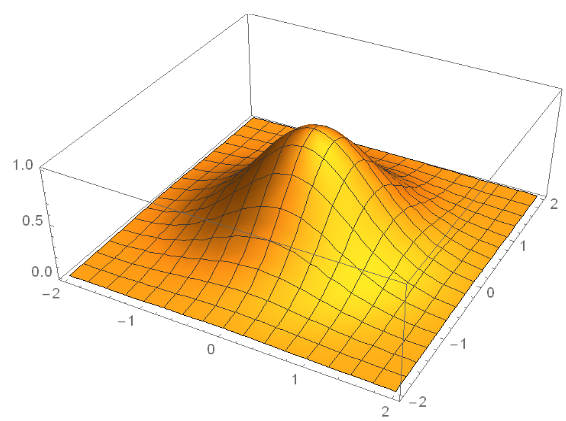

Fig. 3 Variations of absorption to extinction ratio and scattering to an extinction ratio for cerium nanospheres with various radiuses. It should be noted that the x-axis shows cerium nanospheres radius (nanoparticles size) (nm), the y-axis shows absorption and the z-axis shows wavelength (nm).

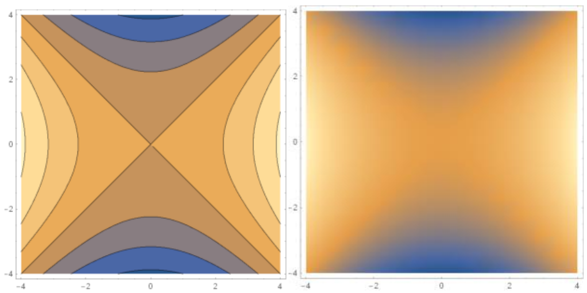

Fig. 4 Maximum increase in temperature for spherical nanoparticles with a radius of 45 nm at plasmon wavelength of 685 nm.

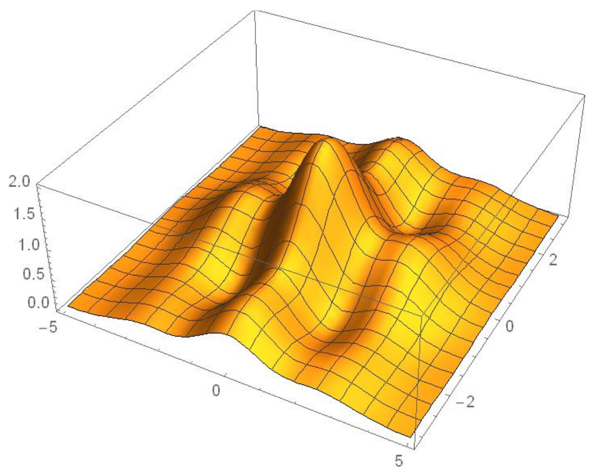

Fig. 5 Maximum increase in temperature for core-shell cerium nanospheres with various thicknesses of the silica shell. It should be noted that the x-axis shows cerium nanospheres radius (nanoparticles size) (nm), the y-axis shows the temperature of nanospheres in surface plasmon frequency (K) and z-axis shows wavelength (nm).

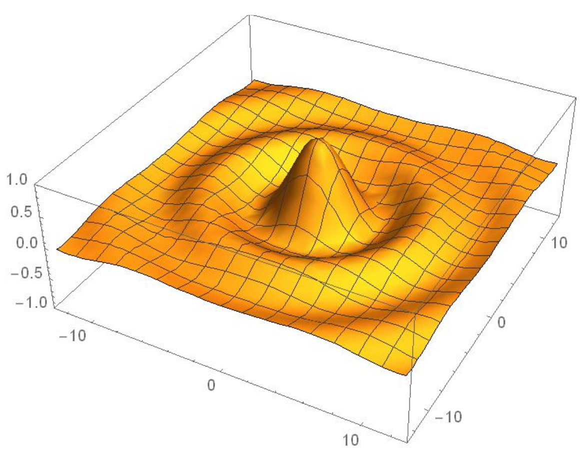

Fig. 6 Maximum increase in temperature for core-shell nanoparticles with a radius of 45 nm and a silica thickness of 10 nm at plasmon wavelength of 701 n). It should be noted that the x-axis shows cerium nanospheres radius (nanoparticles size) (nm), the y-axis shows the temperature of nanospheres in surface plasmon frequency (K) and z-axis shows wavelength (nm).

cross-section area increases and maximum wavelength slightly shifted toward longer wavelengths. The maximum increase in temperature of nanospheres in surface plasmon frequency is shown in Fig. 2. The results showed that the generated heat was increased by the increase in nanoparticles size. For 100 nm nanoparticles (sphere with 50 nm radius), the maximum increase in temperature was 83 K. When nanoparticles size was reached to 150 nm, an increase in temperature was enhanced in spite of the increase in the extinction coefficient.

In order to find the reason for this fact, the ratio of absorption to extinction for various nanospheres in plasmon frequency is shown in Fig. 3. The results showed that increasing the size of nanospheres led to a decrease in the ratio of light absorption to the total energy of descendent light so that for 150 nm nanosphere, scattering was larger than absorption. It seems that despite an increase in nanoparticles size led to more dissipation of descendent light, the dissipation was in the form of scattering and hence, it cannot be effective in heat generation. The results of heat distribution showed that temperature was uniformly distributed throughout the nanoparticles, which was due to the high thermal conductivity of cerium (Fig. 4). In this section, the core-shell structure of cerium and silica was chosen. The core of a nanosphere with a 45 nm radius and silica layer thickness of 5, 10, 15, 20, 25, 30, 35, 40, 45 and 50 nanometers were considered. The results showed that an increase in silica thickness led to an increase in the extinction coefficient and a shift in the plasmon wavelength of nanoparticles, to some extent.

According to Fig. 5, silica shell causes a considerable increase in temperature of cerium nanoparticles but with more increase in silica thickness, its effect was decreased. Heat distribution shows that the temperature was uniformly distributed throughout the metallic core as well as silica shell (Fig. 6). However, silica temperature was considerably lower than the core temperature due to its lower thermal conductivity. In fact, the silica layer prohibits the heat transfer from metal to the surrounding aqueous environment due to low thermal conductivity. Hence, the temperature of nanoparticles has more increase in temperature. Increasing the thickness of the silica shell leads to an increase in its thermal conductivity and leads to attenuation in the increase in nanoparticle temperature. According to Fig. 7, the variation of the nanorod dimension ratio led to a

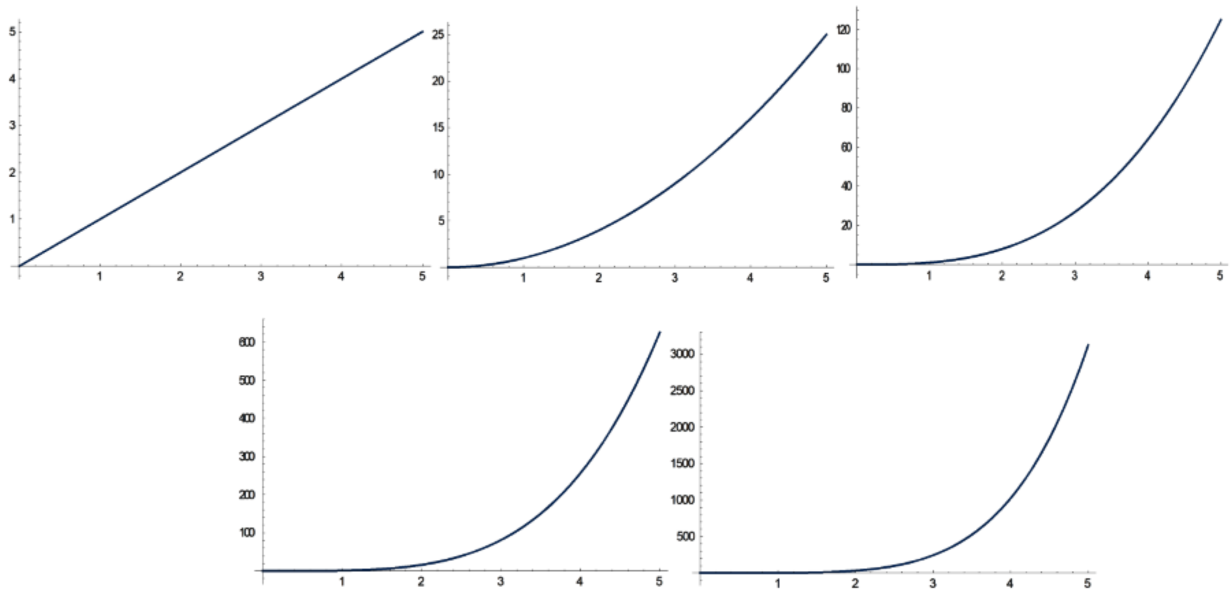

Fig. 7 Extinction cross-section area for cerium nanorods with an effective radius of 45 nm and various dimension ratios.

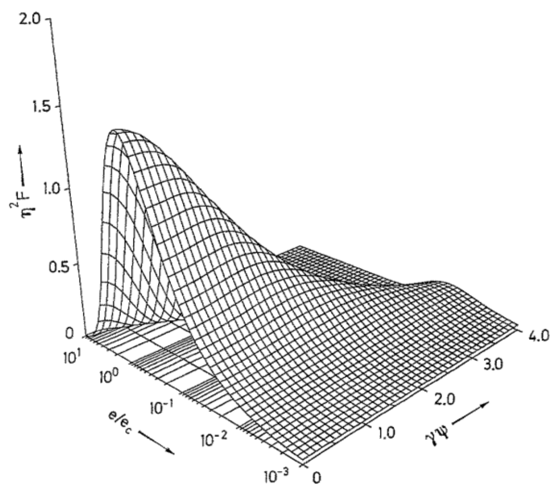

Fig. 8 Spectral and angular distribution of dimensionless synchrotron radiation power per normalized photon energy.

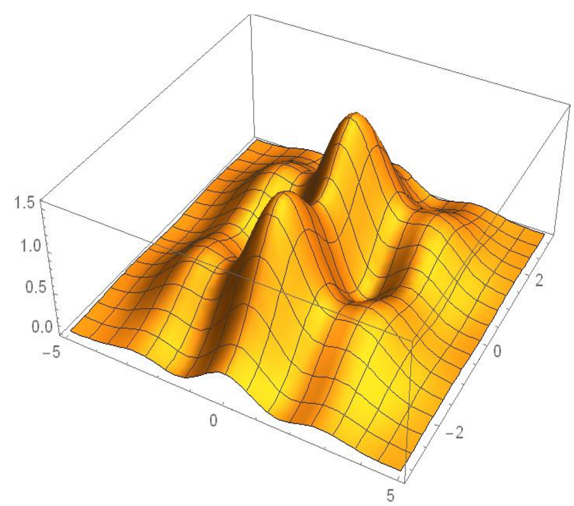

Fig. 9 Maximum increase in temperature for nanorods with an effective radius of 20 nm and 45 nm and various dimension ratios. It should be noted that the x-axis shows the cerium nanospheres radius (nanoparticles size) (nm), the y-axis shows the temperature of nanospheres in surface Plasmon frequency (K) and z-axis shows wavelength (nm).

a considerable shift in plasmon wavelength. This fact allows regulating the plasmon frequency to place in the near IR zone. Light absorption by body tissues was lower in this zone of the spectrum and hence, nanorods are more appropriate for optothermal human cancer cells, tissues and tumors treatment methods. Also, Fig. 8 illustrates spectral and angular distribution of dimensionless synchrotron radiation power per normalized photon energy. Variations of temperature in cerium nanorods with two effective radius and various dimension ratios are shown in Fig. 9. By increase in length (a) to radius (b) of nanorod, the temperature was increased.

Conclusions

The calculations showed that in cerium nanoparticles, light absorption in plasmon frequency cause to increase in temperature of the surrounding environment of nanoparticles. In addition, it shows that adding a thin silica layer around the cerium nanospheres increased their temperature. Calculations of nanorods showed that due to the ability to shift surface plasmon frequency toward longer wavelength as well as more increase in temperature, this nanostructure is more appropriate for medical applications such as optothermal human cancer cells, tissues and tumor treatments.

Acknowledgments

Authors are supported by an American International Standards Institute (AISI) Future Fellowship Grant FT1201009373472. We acknowledge Ms. Isabelle Villena for instrumental support and Dr. Michael N. Cocchi for constructing graphical abstract figures. We gratefully acknowledge Prof. Dr. Christopher Brown for proof reading the manuscript. Synchrotron beam time was awarded by the National Synchrotron Light Source (NSLS–II) under the merit–based proposal scheme.

Conflict of interest

The authors have no conflict of interest.

References

[1] Heidari A, Brown C. Study of composition and morphology of cadmium oxide (CdO) nanoparticles for eliminating cancer cells. J Nanomed Res 2015; 2(5):00042.

[2] Heidari A, Brown C. Study of surface morphological, phytochemical and structural characteristics of rhodium (iii) oxide (Rh_2O_3) nanoparticles. Inter J Pharmacol Phytochem Ethnomed 2015; 1(1):15–19.

[3] Heidari A. An experimental biospectroscopic study on seminal plasma in determination of semen quality for evaluation of male infertility. Int J Adv Technol 2016; 7:e007.

[4] Heidari A. Extraction and preconcentration of n–tolyl–sulfonyl–phosphoramid–saeure–dichlorid as an anti–cancer drug from plants: a pharmacognosy study. J Pharmacogn Nat Prod 2016; 2:e103.

[5] Heidari A. A thermodynamic study on hydration and dehydration of dna and rna−amphiphile complexes. J Bioeng Biomed Sci 2016; S:006.

[6] Heidari A. Computational studies on molecular structures and carbonyl and ketene groups' effects of singlet and triplet energies of azidoketene O=C=CH–NNN and isocyanatoketene O=C=CH–N=C=O. J Appl Computat Math 2016; 5:e142.

[7] Heidari A. Study of irradiations to enhance the induces the dissociation of hydrogen bonds between peptide chains and transition from helix structure to random coil structure using ATR–FTIR, raman and ^{1}HNMR spectroscopies. J Biomol Res Ther 2016; 5:e146.

[8] Heidari A. Future prospects of point fluorescence spectroscopy, fluorescence imaging and fluorescence endoscopy in photodynamic therapy (PDT) for cancer cells. J Bioanal Biomed 2016; 8: e135.

[9] Heidari A. A bio–spectroscopic study of dna density and color role as determining factor for absorbed irradiation in cancer cells. Adv Cancer Prev 2016; 1:e102.

[10] Heidari A. Manufacturing process of solar cells using cadmium oxide (CdO) and rhodium (III) oxide (Rh_2O_3) nanoparticles. J Biotechnol Biomater 2016; 6:e125.

[11] Heidari A. A novel experimental and computational approach to photobiosimulation of telomeric DNA/RNA: a biospectroscopic and photobiological study. J Res Development 2016; 4:1000144.

[12] Heidari A. Biochemical and pharmacodynamical study of microporous molecularly imprinted polymer selective for vancomycin, teicoplanin, oritavancin, telavancin and dalbavancin binding. 2016; Biochem Physiol 5:e146.

[13] Heidari A. Anti–cancer effect of uv irradiation at presence of cadmium oxide (CdO) nanoparticles on dna of cancer cells: a photodynamic therapy study. Arch Cancer Res 2016; 4:1.

[14] Heidari A. Biospectroscopic study on multi–component reactions (MCRs) in two A–type and B–type conformations of nucleic acids to determine ligand binding modes, binding constant and stability of nucleic acids in cadmium oxide (CdO) nanoparticles–nucleic acids complexes as anti–cancer drugs. Arch Cancer Res 2016; 4:2.

[15] Heidari A. Simulation of temperature distribution of DNA/RNA of human cancer cells using time–dependent bio–heat equation and nd: YAG lasers. Arch Cancer Res 2016; 4:2.

[16] Heidari A. Quantitative structure–activity relationship (QSAR) approximation for cadmium oxide (CdO) and rhodium (III) oxide (Rh_2O_3) nanoparticles as anti–cancer drugs for the catalytic formation of proviral DNA from viral RNA using multiple linear and non–linear correlation approach. Ann Clin Lab Res 2016; 4:1.

[17] Heidari A. Biomedical study of cancer cells DNA therapy using laser irradiations at presence of intelligent nanoparticles. J Biomedical Sci 2016; 5:2.

[18] Heidari A. Measurement the amount of vitamin D2 (ergocalciferol), vitamin D3 (cholecalciferol) and absorbable calcium (Ca^{2+}), iron (II) (Fe^{2+}), magnesium (Mg^{2+}), phosphate (PO^{4-}) and zinc (Zn^{2+}) in apricot using high–performance liquid chromatography (HPLC) and spectroscopic techniques. J Biom Biostat 2016; 7:292.

[19] Heidari A. Spectroscopy and quantum mechanics of the helium dimer (He^{2+}), neon dimer (Ne^{2+}), argon dimer (Ar^{2+}), krypton dimer (Kr^{2+}), xenon dimer (Xe^{2+}), radon dimer (Rn^{2+}) and ununoctium dimer (Uuo^{2+}) molecular cations", Chem Sci J 2016; 7:e112.

[20] Heidari A. Human toxicity photodynamic therapy studies on DNA/RNA complexes as a promising new sensitizer for the treatment of malignant tumors using bio–spectroscopic techniques. J Drug Metab Toxicol 2016; 7:e129.

[21] Heidari A. Novel and stable modifications of intelligent cadmium oxide (CdO) nanoparticles as anti–cancer drug in formation of nucleic acids complexes for human cancer cells' treatment. Biochem Pharmacol 2016; 5:207.

[22] Heidari A. A combined computational and QM/MM molecular dynamics study on boron nitride nanotubes (BNNTs), amorphous boron nitride nanotubes (a–BNNTs) and hexagonal boron nitride nanotubes (h–BNNTs) as hydrogen storage. Struct Chem Crystallogr Commun 2016; 2:1.

[23] Heidari A. Pharmaceutical and analytical chemistry study of cadmium oxide (CdO) nanoparticles synthesis methods and properties as anti–cancer drug and its effect on human cancer cells. Pharm Anal Chem 2016; 2:113.

[24] Heidari A. A chemotherapeutic and biospectroscopic investigation of the interaction of double–standard DNA/RNA–binding molecules with cadmium oxide (CdO) and rhodium (III) oxide (Rh_2O_3) nanoparticles as anti–cancer drugs for cancer cells treatment. Chemo Open Access 2016; 5:e129.

[25] Heidari A. Pharmacokinetics and experimental therapeutic study of dna and other biomolecules using lasers: advantages and applications. J Pharmacokinet Exp Ther 2016; 1:e005.

[26] Heidari A. Determination of ratio and stability constant of DNA/RNA in human cancer cells and cadmium oxide (CdO) nanoparticles complexes using analytical electrochemical and spectroscopic techniques. Insights Anal Electrochem 2016; 2:1.

[27] Heidari A. Discriminate between antibacterial and non–antibacterial drugs artificial neutral networks of a multilayer perceptron (MLP) type using a set of topological descriptors. J Heavy Met Toxicity Dis 2016; 1:2.

[28] Heidari A. Combined theoretical and computational study of the belousov–zhabotinsky chaotic reaction and curtius rearrangement for synthesis of mechlorethamine, cisplatin, streptozotocin, cyclophosphamide, melphalan, busulphan and BCNU as anti–cancer drugs. Insights Med Phys. 2016; 1:2.

[29] Heidari A. A translational biomedical approach to structural arrangement of amino acids' complexes: a combined theoretical and computational study. Transl Biomed. 2016; 7:2.

[30] Heidari A. Ab initio and density functional theory (DFT) studies of dynamic NMR shielding tensors and vibrational frequencies of DNA/RNA and cadmium oxide (CdO) nanoparticles complexes in human cancer cells. J Nanomedine Biotherapeutic Discov 2016; 6:e144.

[31] Heidari A. Molecular dynamics and Monte–Carlo simulations for replacement sugars in insulin resistance, obesity, LDL cholesterol, triglycerides, metabolic syndrome, type 2 diabetes and cardiovascular disease: A glycobiological study. J Glycobiol 2016; 5:e111.

[32] Heidari A. Synthesis and study of 5–[(phenylsulfonyl)amino]–1,3,4–thiadiazole–2–sulfonamide as potential anti–pertussis drug using chromatography and spectroscopy techniques. Transl Med (Sunnyvale) 2016; 6:e138.

[33] Heidari A. Nitrogen, oxygen, phosphorus and sulphur heterocyclic anti–cancer nano drugs separation in the supercritical fluid of ozone (O_3) using soave–redlich–kwong (SRK) and pang–robinson (PR) equations. Electronic J Biol 2016; 12:4.

[34] Heidari A. An analytical and computational infrared spectroscopic review of vibrational modes in nucleic acids. Austin J Anal Pharm Chem 2016; 3(1):1058.

[35] Heidari A. Brown C. Phase, composition and morphology study and analysis of Os–Pd/HfC nanocomposites. Nano Res Appl 2016; 2(1):14.

[36] Heidari A, Brown C. Vibrational spectroscopic study of intensities and shifts of symmetric vibration modes of ozone diluted by cumene. Int J Adv Chem 2016; 4(1):5–9.

[37] Heidari A. Study of the role of anti–cancer molecules with different sizes for decreasing corresponding bulk tumor multiple organs or tissues. Arch Can Res 2016; 4(2):83.

[38] Heidari A. Genomics and proteomics studies of zolpidem, necopidem, alpidem, saripidem, miroprofen, zolimidine, olprinone and abafungin as anti–tumor, peptide antibiotics, antiviral and central nervous system (CNS) drugs. J Data Mining GenomProteom 2016; 7:e125.

[39] Heidari A. Pharmacogenomics and pharmacoproteomics studies of phosphodiesterase–5 (PDE5) inhibitors and paclitaxel albumin–stabilized nanoparticles as sandwiched anti–cancer nano drugs between two DNA/RNA molecules of human cancer cells. J Pharmacogen Pharmacoprot 2016; 7:e153.

[40] Heidari A. Biotranslational medical and biospectroscopic studies of cadmium oxide (CdO) nanoparticles–DNA/RNA straight and cycle chain complexes as potent anti–viral, anti–tumor and anti–microbial drugs: a clinical approach. Transl Biomed 2016; 4(2):76.

[41] Heidari A. A comparative study on simultaneous determination and separation of adsorbed cadmium oxide (CdO) nanoparticles on DNA/RNA of human cancer cells using biospectroscopic techniques and dielectrophoresis (DEP) method. Arch Can Res 2016; 4(2):86.

[42] Heidari A. Cheminformatics and system chemistry of cisplatin, carboplatin, nedaplatin, oxaliplatin, heptaplatin and lobaplatin as anti–cancer nano drugs: a combined computational and experimental study. J Inform Data Min 2016; 1(3):15.

[43] Heidari A. Linear and non–linear quantitative structure–anti–cancer–activity relationship (QSACAR) study of hydrous ruthenium (IV) oxide (RuO_2) nanoparticles as non–nucleoside reverse transcriptase inhibitors (NNRTIs) and anti–cancer nano drugs. J Integr 2016; Oncol 5:e110.

[44] Heidari A. Synthesis, characterization and biospectroscopic studies of cadmium oxide (CdO) nanoparticles–nucleic acids complexes absence of soluble polymer as a protective agent using nucleic acids condensation and solution reduction method. J Nanosci Curr Res 2016; 1:e101.

[45] Heidari A. Coplanarity and collinearity of 4'–dinonyl–2,2'–bithiazole in one domain of bleomycin and pingyangmycin to be responsible for binding of cadmium oxide (CdO) nanoparticles to DNA/RNA bidentate ligands as anti–tumor nano drug. Int J Drug Dev Res 2016; 8:7–8.

[46] Heidari A. A pharmacovigilance study on linear and non–linear quantitative structure (chromatographic) retention relationships (QSRR) models for the prediction of retention time of anti–cancer nano drugs under synchrotron radiations. J Pharmacovigil 2016; 4:e161.
[47] Heidari A. Nanotechnology in preparation of semipermeable polymers. J Adv Chem Eng 2016; 6:157.
[48] Heidari A. A gastrointestinal study on linear and non–linear quantitative structure (chromatographic) retention relationships (QSRR) models for analysis 5–aminosalicylates nano particles as digestive system nano drugs under synchrotron radiations. J Gastrointest Dig Syst 2016; 6:e119.
[49] Heidari A. DNA/RNA fragmentation and cytolysis in human cancer cells treated with diphthamide nano particles derivatives. Biomedical Data Mining 2016; 5:e102.
[50] Heidari A. A successful strategy for the prediction of solubility in the construction of quantitative structure–activity relationship (QSAR) and quantitative structure–property relationship (QSPR) under synchrotron radiations using genetic function approximation (GFA) algorithm. J Mol Biol Biotechnol 2016; 1:1.
[51] Heidari A. Computational study on molecular structures of C_{20}, C_{60}, C_{240}, C_{540}, C_{960}, C_{2160} and C_{3840} fullerene nano molecules under synchrotron radiations using fuzzy logic. J Material Sci Eng 2016; 5:282.
[52] Heidari A. Graph theoretical analysis of zigzag polyhexamethylene biguanide, polyhexamethylene adipamide, polyhexamethylene biguanide gauze and polyhexamethylene biguanide hydrochloride (PHMB) boron nitride nanotubes (BNNTs), amorphous boron nitride nanotubes (a–BNNTs) and hexagonal boron nitride nanotubes (h–BNNTs). J Appl Computat Math 2016; 5:e143.
[53] Heidari A. The impact of high resolution imaging on diagnosis. Int J Clin Med Imaging 2016; 3:1000e101.
[54] Heidari A. A comparative study of conformational behavior of isotretinoin (13–Cis retinoic acid) and tretinoin (all–trans retinoic acid (ATRA)) nano particles as anti–cancer nano drugs under synchrotron radiations using hartree–fock (HF) and density functional theory (DFT) methods. Insights in Biomed 2016; 1:2.
[55] Heidari A. Advances in logic, operations and computational mathematics. J Appl Computat Math 2016; 5:5.
[56] Heidari A. Mathematical equations in predicting physical behavior. J Appl Computat Math 2016; 5:5.
[57] Heidari A. Chemotherapy a last resort for cancer treatment. Chemo Open Access 2016; 5:4.
[58] Heidari A. Separation and pre–concentration of metal cations–DNA/RNA chelates using molecular beam mass spectrometry with tunable vacuum ultraviolet (VUV) synchrotron radiation and various analytical methods. Mass Spectrom Purif Tech 2016; 2:e101.
[59] Heidari A. Yoctosecond quantitative structure–activity relationship (QSAR) and quantitative structure–property relationship (QSPR) under synchrotron radiations studies for prediction of solubility of anti–cancer nano drugs in aqueous solutions using genetic function approximation (GFA) algorithm. Insight Pharm Res 2016; 1:1.
[60] Heidari A. Cancer risk prediction and assessment in human cells under synchrotron radiations using quantitative structure activity relationship (QSAR) and quantitative structure properties relationship (QSPR) studies. Int J Clin Med Imaging 2016; 3:516.
[61] Heidari A. A novel approach to biology. Electronic J Biol 2016; 12:4.
[62] Heidari A. Innovative biomedical equipment's for diagnosis and treatment. J Bioengineer Biomedical Sci 2016; 6:2.
[63] Heidari A. Integrating precision cancer medicine into healthcare, medicare reimbursement changes and the practice of oncology: trends in oncology medicine and practices. J Oncol Med Pract 2016; 1:2.
[64] Heidari A. Promoting convergence in biomedical and biomaterials sciences and silk proteins for biomedical and biomaterials applications: an introduction to materials in medicine and bioengineering perspectives. J Bioengineer Biomedical Sci 2016; 6:3.
[65] Heidari A. X–Ray fluorescence and x–ray diffraction analysis on discrete element modeling of nano powder metallurgy processes in optimal container design. J Powder Metall Min 2017; 6:1.
[66] Heidari A. Biomolecular spectroscopy and dynamics of nano–sized molecules and clusters as cross–linking–induced anti–cancer and immune–oncology nano drugs delivery in DNA/RNA of human cancer cells' membranes under synchrotron radiations: a payload–based perspective. Arch Chem Res 2017; 1:2.
[67] Heidari A. Deficiencies in Repair of Double–Standard DNA/RNA–Binding Molecules Identified in Many Types of Solid and Liquid Tumors Oncology in Human Body for Advancing Cancer Immunotherapy Using Computer Simulations and Data Analysis: Number of Mutations in a Synchronous Tumor Varies by Age and Type of Synchronous Cancer. J Appl Bioinforma Comput Biol 2017; 6:1.
[68] Heidari A. Electronic coupling among the five nanomolecules shuts down quantum tunneling in the presence and absence of an applied magnetic field for indication of the dimer or other provide different influences on the magnetic behavior of single molecular magnets (SMMs) as qubits for quantum computing. Glob J Res Rev 2017; 4:2.
[69] Heidari A. Polymorphism in nano–sized graphene ligand–induced transformation of Au_{38}–$xAg_x/xCu_x(SPh–tBu)_{24}$ to Au_{36}–$xAg_x/xCu_x(SPh–tBu)_{24}$ (x = 1–12) Nanomolecules for synthesis of Au_{144}–$xAg_x/xCu_x[(SR)_{60}$, $(SC_4)_{60}$, $(SC_6)_{60}$, $(SC_{12})_{60}$, $(PET)_{60}$, $(p–MBA)_{60}$, $(F)_{60}$, $(Cl)_{60}$, $(Br)_{60}$, $(I)_{60}$, $(At)_{60}$, $(Uus)_{60}$ and $(SC_6H_{13})_{60}]$ nano clusters as anti–cancer nano drugs. J Nanomater Mol Nanotechnol 2017; 6:3.
[70] Heidari A. Biomedical resource oncology and data mining to enable resource discovery in medical, medicinal, clinical, pharmaceutical, chemical and translational research and their applications in cancer research. Int J Biomed Data Min 2017; 6:e103.
[71] Heidari A. Study of synthesis, pharmacokinetics, pharmacodynamics, dosing, stability, safety and efficacy of olympiadane nanomolecules as agent for

cancer enzymotherapy, immunotherapy, chemotherapy, adiotherapy, hormone therapy and targeted therapy under synchrotorn radiation. J Dev Drugs 2017; 6:e154.
[72] Heidari A. A novel approach to future horizon of top seven biomedical research topics to watch in 2017: alzheimer's, ebola, hypersomnia, human immunodeficiency virus (HIV), tuberculosis (TB), microbiome/antibiotic resistance and endovascular stroke. J Bioengineer Biomedical Sci 2017; 7:e127.
[73] Heidari A. Opinion on computational fluid dynamics (CFD) technique. Fluid Mech Open Acc 2017; 4:157.
[74] Heidari A. Concurrent diagnosis of oncology influence outcomes in emergency general surgery for colorectal cancer and multiple sclerosis (MS) treatment using magnetic resonance imaging (MRI) and $Au_{329}(SR)_{84}$, $Au_{329-x}Ag_x(SR)_{84}$, $Au_{144}(SR)_{60}$, $Au_{68}(SR)_{36}$, $Au_{30}(SR)_{18}$, $Au_{102}(SPh)_{44}$, $Au_{38}(SPh)_{24}$, $Au_{38}(SC_2H_4Ph)_{24}$, $Au_{21}S(SAdm)_{15}$, $Au_{36}(pMBA)_{24}$ and $Au_{25}(pMBA)_{18}$ nano clusters. J Surgery Emerg Med 2017; 1:21.
[75] Heidari A. developmental cell biology in adult stem cells death and autophagy to trigger a preventive allergic reaction to common airborne allergens under synchrotron radiation using nanotechnology for therapeutic goals in particular allergy shots (immunotherapy). Cell Biol 2017; 6:1.
[76] Heidari A. Changing metal powder characteristics for elimination of the heavy metals toxicity and diseases in disruption of extracellular matrix (ECM) proteins adjustment in cancer metastases induced by osteosarcoma, chondrosarcoma, carcinoid, carcinoma, ewing's sarcoma, fibrosarcoma and secondary hematopoietic solid or soft tissue tumors. J Powder Metall Min 2017; 6:170.
[77] Heidari A. Nanomedicine–based combination anti–cancer therapy between nucleic acids and anti–cancer nano drugs in covalent nano drugs delivery systems for selective imaging and treatment of human brain tumors using hyaluronic acid, alguronic acid and sodium hyaluronate as anti–cancer nano drugs and nucleic acids delivery under synchrotron radiation. Am J Drug Deliv 2017; 5:2.
[78] Heidari A. Clinical trials of dendritic cell therapies for cancer exposing vulnerabilities in human cancer cells' metabolism and metabolomics: new discoveries, unique features inform new therapeutic opportunities, biotech's bumpy road to the market and elucidating the biochemical programs that support cancer initiation and progression. J Biol Med Science 2017; 1:e103.
[79] Heidari A. The design graphene–based nanosheets as a new nanomaterial in anti–cancer therapy and delivery of chemotherapeutics and biological nano drugs for liposomal anti–cancer nano drugs and gene delivery. Br Biomed Bull 2017; 5:305.
[80] Heidari A. Integrative approach to biological networks for emerging roles of proteomics, genomics and transcriptomics in the discovery and validation of human colorectal cancer biomarkers from DNA/RNA sequencing data under synchrotron radiation. Transcriptomics 2017; 5:e117.
[81] Heidari A. Elimination of the heavy metals toxicity and diseases in disruption of extracellular matrix (ECM) proteins and cell adhesion intelligent nanomolecules adjustment in cancer metastases using metalloenzymes and under synchrotron radiation. Lett Health Biol Sci 2017; 2 (2):1–4.
[82] Heidari A. Treatment of breast cancer brain metastases through a targeted nanomolecule drug delivery system based on dopamine functionalized multi–wall carbon nanotubes (MWCNTs) coated with nano graphene oxide (GO) and protonated polyaniline (pani) in situ during the polymerization of aniline autogenic nanoparticles for the delivery of anti–cancer nano drugs under synchrotron radiation. Br J Res 2017; 4(3):16.
[83] Heidari A. Sedative, analgesic and ultrasound–mediated gastrointestinal nano drugs delivery for gastrointestinal endoscopic procedure, nano drug–induced gastrointestinal disorders and nano drug treatment of gastric acidity. Res Rep Gastroenterol 2017; 1:1.
[84] Heidari A. Synthesis, pharmacokinetics, pharmacodynamics, dosing, stability, safety and efficacy of orphan nano drugs to treat high cholesterol and related conditions and to prevent cardiovascular disease under synchrotron radiation. J Pharm Sci Emerg Drugs 2017; 5:1.
[85] Heidari A. Non–linear compact proton synchrotrons to improve human cancer cells and tissues treatments and diagnostics through particle therapy accelerators with monochromatic microbeams. J Cell Biol Mol Sci 2017; 2(1):1–5.
[86] Heidari A. Design of targeted metal chelation therapeutics nanocapsules as colloidal carriers and blood–brain barrier (BBB) translocation to targeted deliver anti–cancer nano drugs into the human brain to treat alzheimer's disease under synchrotron radiation. J Nanotechnol Material Sci 2017; 4(2):1–5.
[87] Gobato R, Heidari A. Calculations using quantum chemistry for inorganic molecule simulation $BeLi_2SeSi$. Sci J Analy Chem 2017; 5(6):76–85.
[88] Heidari A. Different high–resolution simulations of medical, medicinal, clinical, pharmaceutical and therapeutics oncology of human lung cancer translational anti–cancer nano drugs delivery treatment process under synchrotron and X–ray radiations. J Med Oncol 2017; 1:1.
[89] Heidari A. A modern ethnomedicinal technique for transformation, prevention and treatment of human malignant gliomas tumors into human benign gliomas tumors under synchrotron radiation. Am J Ethnomed 2017; 4(1):10.
[90] Heidari A. Active targeted nanoparticles for anti–cancer nano drugs delivery across the blood–brain barrier for human brain cancer treatment, multiple sclerosis (MS) and Alzheimer's diseases using chemical modifications of anti–cancer nano drugs or drug–nanoparticles through zika virus (ZIKV) nanocarriers under synchrotron radiation. J Med Chem Toxicol 2017; 2(3):1–5.
[91] Heidari A. Investigation of medical, medicinal, clinical and pharmaceutical applications of estradiol, mestranol (norlutin), norethindrone (NET), norethisterone acetate (NETA), norethisterone enanthate (NETE) and testosterone nanoparticles as biological imaging, cell labeling, anti–microbial agents and anti–cancer nano

drugs in nanomedicines based drug delivery systems for anti–cancer targeting and treatment. Parana J Sci Edu 2017; 3(4):10–19.

[92] Heidari A. A comparative computational and experimental study on different vibrational biospectroscopy methods, techniques and applications for human cancer cells in tumor tissues simulation, modeling, research, diagnosis and treatment. Open J Anal Bioanal Chem 2017; 1(1):14–20.

[93] Heidari A. Combination of DNA/RNA ligands and linear/non–linear visible–synchrotron radiation–driven n–doped ordered mesoporous cadmium oxide (CdO) nanoparticles photocatalysts channels resulted in an interesting synergistic effect enhancing catalytic anti–cancer activity. Enz Eng 2017; 6:1.

[94] Heidari A. Modern approaches in designing ferritin, ferritin light chain, transferrin, beta–2 transferrin and bacterioferritin–based anti–cancer nano drugs encapsulating nanosphere as DNA–binding proteins from starved cells (DPS). Mod Appro Drug Des 2017; 1:1.

[95] Heidari A. Potency of human interferon β–1a and human interferon β–1b in enzymotherapy, immunotherapy, chemotherapy, radiotherapy, hormone therapy and targeted therapy of encephalomyelitis disseminate/multiple sclerosis (ms) and hepatitis A, B, C, D, E, F and G virus enter and targets liver cells. J Proteomics Enzymol 2017; 6:1.

[96] Heidari A. Transport therapeutic active targeting of human brain tumors enable anti–cancer nanodrugs delivery across the blood–brain barrier (BBB) to treat brain diseases using nanoparticles and nanocarriers under synchrotron radiation. J Pharm Pharmaceutics 2017; 4(2):1–5.

[97] Heidari A. Brown C. Combinatorial therapeutic approaches to DNA/RNA and benzylpenicillin (penicillin G), fluoxetine hydrochloride (prozac and sarafem), propofol (Diprivan), acetylsalicylic aacid (ASA) (aspirin), naproxen Sodium (aleve and naprosyn) and dextromethamphetamine nanocapsules with surface conjugated DNA/RNA to targeted nano drugs for enhanced anti–cancer efficacy and targeted cancer therapy using nano drugs delivery systems", Ann Adv Chem. 2017; 1(2):61–69.

[98] Heidari A. High–resolution simulations of human brain cancer translational nano drugs delivery treatment process under synchrotron radiation. J Transl Res 2017; 1(1):1–3.

[99] Heidari A. Investigation of anti–cancer nano drugs' effects' trend on human pancreas cancer cells and tissues prevention, diagnosis and treatment process under synchrotron and X–ray radiations with the passage of time using Mathematica. Current Trends Anal Bioanal Chem 2017; 1(1):36–41.

[100] Heidari A. Pros and cons controversy on molecular imaging and dynamics of double–standard DNA/RNA of human preserving stem cells–binding nano molecules with androgens/anabolic steroids (aas) or testosterone derivatives through tracking of helium–4 nucleus (alpha particle) using synchrotron radiation. Arch Biotechnol Biomed 2017; 1(1):67–100.

[101] Heidari A. Visualizing metabolic changes in probing human cancer cells and tissues metabolism using vivo ^{1}H or proton NMR, ^{13}C NMR, ^{15}N NMR and ^{31}P NMR spectroscopy and self–organizing maps under synchrotron radiation. SOJ Mater Sci Eng 2017; 5(2):1–6.

[102] Heidari A. Cavity ring–down spectroscopy (CRDS), circular dichroism spectroscopy, cold vapour atomic fluorescence spectroscopy and correlation spectroscopy comparative study on malignant and benign human cancer cells and tissues with the passage of time under synchrotron radiation. Enliven: Challenges Cancer Detect Ther 2017; 4(2):e001.

[103] Heidari A. Laser spectroscopy, laser–induced breakdown spectroscopy and laser–induced plasma spectroscopy comparative study on malignant and benign human cancer cells and tissues with the passage of time under synchrotron radiation. Int J Hepatol Gastroenterol 2017; 3(4):79–84.

[104] Heidari A. Time–resolved spectroscopy and time–stretch spectroscopy comparative study on malignant and benign human cancer cells and tissues with the passage of time under synchrotron radiation. Enliven: Pharmacovig Drug Safe 2017; 4(2):e001.

[105] Heidari A. Overview of the role of vitamins in reducing negative effect of decapeptyl (triptorelin acetate or pamoate salts) on prostate cancer cells and tissues in prostate cancer treatment process through transformation of malignant prostate tumors into benign prostate tumors under synchrotron radiation. Open J Anal Bioanal Chem 2017; 1(1):21–26.

[106] Heidari A. Electron phenomenological spectroscopy, electron paramagnetic resonance (EPR) spectroscopy and electron spin resonance (ESR) spectroscopy comparative study on malignant and benign human cancer cells and tissues with the passage of time under synchrotron radiation. Austin J Anal Pharm Chem 2017; 4(3):1091.

[107] Heidari A. Therapeutic nanomedicine different high–resolution experimental images and computational simulations for human brain cancer cells and tissues using nanocarriers deliver DNA/RNA to brain tumors under synchrotron radiation with the passage of time using mathematica and MATLAB. Madridge J Nano Tech Sci 2017; 2(2):77–83.

[108] Kashi ASY, Khaledi S, Houshyari M. CT simulation to evaluate of pelvic lymph node coverage in conventional radiotherapy fields based on bone and vessels landmarks in prostate cancer patients. Iran J Cancer Prev 2016; 9(3):e6233.

[109] Kashi ASY, Razzaghdoust A, Rakhsha A. A comparative study of treatment toxicities between FOLFOX 4 and modified FOLFOX 6 in Iranian colorectal cancer patients. Iran J Cancer Prev 2017; 10(1):e9429.

[110] Kashi ASY, YazdanfarS, Akbari ME, Rakhsha A. Triple negative breast cancer in iranian women: clinical profile and survival study. Int J Cancer Manag 2017; 10(8):e10471.

[111] Kashi ASY, Montazeri R, Rakhsha A. clinical outcome and prognostic factors in iranian breast cancer patients

after neoadjuvant chemotherapy: a comparative matched study. Int J Cancer Manag 2018; 11(5):e67739.
[112] Rakhsha A, Anvari A, Razzaghdoust A, Kashi ASY. Clinical outcome and prognostic factors for very young patients with breast cancer: a comparative matched single institution study in Iran. Int J Cancer Manag 2017; 10(9):e11772.
[113] Rakhsha A, Kashi ASY, Hoseini SM. Evaluation of survival and treatment toxicity with high–dose–rate brachytherapy with cobalt 60 in carcinoma of cervix. Iran J Cancer Preven 2015; 8(4):e3573.
[114] Kashi ASY, Mofid B, Mirzaei HR, Azadeh P. Overall survival and related prognostic factors in metastatic brain tumors treated with whole brain radiation therapy. Res J Med Sci 2010; 4(3):213–216.